# Chapter 5
# A Dual pH- and Redox-Responsive Phthalocyanine-Based Photosensitizer for Targeted Photodynamic Therapy

## 5.1 Introduction

As mentioned in Chap. 1 (Sect. 1.3.2), different cancer-related stimuli have been explored to "turn on" the activatable photosensitizers with a view to controlling their photodynamic actions. One of the unique features of tumors is their highly reducing environment as compared to normal tissues due to an elevated level of glutathione (GSH) [4, 6, 15]. In Chap. 4, we have described a redox-responsive silicon(IV) phthalocyanine and evaluated the effect of the reductive stimulus on its photophysical properties and in vitro photodynamic activity. In response to a reducing condition analogous to tumor environment, it shows a significant enhancement in fluorescence intensity, singlet oxygen generation efficiency, and photocytotoxicity as a result of reductive cleavage of the disulfide bonds. Another special characteristic of tumors is their relatively low pH in the extracellular region (ca. 6.8) compared with that around normal tissues (ca. 7.3) [11, 27]. The pH-dependent behavior of several classes of photosensitizers, such as porphyrins [7–9, 19], chlorins [7–9, 19, 20, 24, 25], chalcogenopyrylium dyes [3], and phenylene vinylenes [1], has been briefly examined. Recently, we have reported a series of pH-responsive silicon(IV) phthalocyanines substituted with amino moieties in which their photosensitizing properties are greatly enhanced at lower pH, mainly due to protonation of the amino groups which inhibits the intramolecular photo-induced electron transfer (PET) process [14, 16].

The aforementioned examples have vividly demonstrated the use of a single stimulus for photosensitizer activation. In fact, another promising approach is to use two stimuli for the activation of photosensitizer in which the photosensitizer can be fully turned on only when it is exposed to two stimuli concurrently. To this end, Akkaya et al. have reported a boron dipyrromethene (BODIPY)-based activatable photosensitizer in which it exhibits about 6-fold increase in singlet oxygen generation at low pH and high concentration of sodium ion, but no increase in either low pH or high concentration of sodium ion [21]. In addition, dual pH- and redox-sensitive micelles [5] and microcapsules [10] for pinpointed intracellular delivery of anticancer drugs have also been developed. The anticancer drugs are

J. T. F. Lau, *Towards Dual and Targeted Cancer Therapy with Novel Phthalocyanine-based Photosensitizers*, Springer Theses,
DOI: 10.1007/978-3-319-00708-3_5, 

effectively released due to the carrier's susceptible nature to both intracellular reduction and low pH conditions after internalization by tumor cells.

As an extension of our work described in Chap. 4, we have designed a novel dual pH- and redox-responsive phthalocyanine-based activatable photosensitizer. The preparation and basic photophysical properties of this compound, as well as the effect of the pH and reducing stimulus on its in vitro properties are described in this chapter.

## 5.2 Results and Discussion

### *5.2.1 Molecular Design, Synthesis, and Characterization*

In order to confer a redox-responsive property to the phthalocyanine, the ferrocenyl-chalcone ligand **4.9a** (see Chap. 4) was introduced to one of the axial positions. To further incorporate a pH-responsive property to the same phthalocyanine, another ferrocenyl ligand **5.8** was conjugated to the macrocycle through an acid-labile hydrazone linker, which can be selectively cleaved under acidic conditions with pH ranging from 5 to 6 [2]. It is anticipated that the photosensitizing property of the phthalocyanine is inhibited by the ferrocenyl moieties when they are in close proximity. However, when it is exposed to a highly reducing and acidic environment as in the tumor tissues, the disulfide and hydrazone linkers of this compound are expected to be cleaved favorably, thus restoring the photosensitizing property.

Scheme 5.1 shows the synthesis of the acid-labile ferrocenyl carbonyl hydrazone ligand **5.8**. Starting with the commercially available 3,5-dihydroxybenzoic acid (**5.1**), it was first esterificated to methyl 3,5-dihydroxybenzoate (**5.2**) with the aid of a catalytic amount of $H_2SO_4$ and methanol [26]. It was then reduced by lithium aluminium hydride ($LiAlH_4$) in anhydrous tetrahydrofuran (THF) to give 3, 5-dihydroxybenzyl alcohol (**5.3**) [17]. One equiv. of ethyl bromoacetate (**4.5**) was allowed to react with 1 equiv. of alcohol **5.3** in the presence of anhydrous potassium carbonate and acetone to afford the monosubstituted product **5.4**. To enhance the solubility and reduce the aggregation tendency of the phthalocyanine before and after cleavage of both disulfide and hydrazone linkers, a triethylene glycol monomethyl ether chain was introduced by treating **5.4** with tosylate **5.5** [22] to give compound **5.6**. Treatment of hydrazine hydrate with ester **5.6** in ethanol gave hydrazine **5.7** in good yield, which further reacted with ferrocenecarboyaldehyde (**4.2**) in refluxing ethanol to give the ferrocenylcarbonylhydrazone ligand **5.8**.

Scheme 5.2 shows the synthetic route for the preparation of the unsymmetrical phthalocyanine **5.9**. The readily available silicon(IV) phthalocyanine dichloride (**4.10**) was first refluxed with alcohol **4.9a** in the presence of excess pyridine in toluene for 2 h, prior to the addition of ferrocenylcarbonylhydrazone **5.8**. The reaction mixture was continued to reflux for another 4 h to give the unsymmetrical phthalocyanine **5.9** in 15 % yield. Apart from the unsymmetrical phthalocyanine

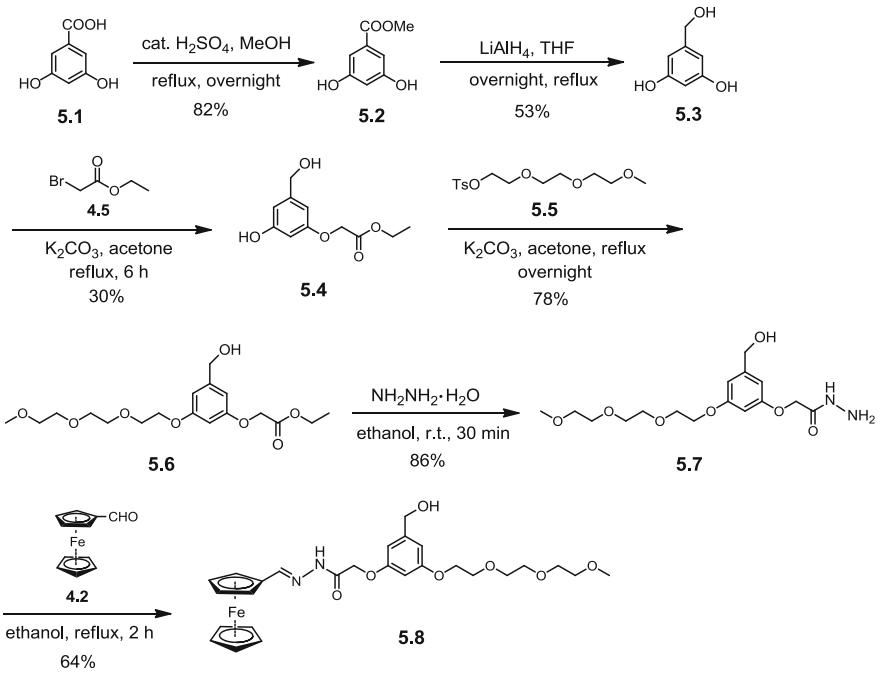


**Scheme 5.1** Synthesis of ferrocenylcarbonylhydrazone **5.8**

**5.9**, a considerable amount of the symmetrical phthalocyanine **5.10** was also isolated in 43 % yield. In view of the potential pH-responsive property of this compound, we also included it in the following study. This compound was also prepared by treating ferrocenylcarbonylhydrazone **5.8** with phthalocyanine **4.10** under a similar reaction condition (Scheme 5.3). As expected, the reaction led to a higher yield (79 %) of **5.10**.

All the new compounds were fully characterized with various spectroscopic methods. Figure 5.1 shows the $^1$H NMR spectrum of **5.9** in $CDCl_3$. It shows two AA′BB′ downfield multiplets at $\delta$ 9.61–9.63 and 8.33–8.35 (8H each), which are assigned to the phthalocyanine $\alpha$- and $\beta$-ring protons, respectively. For the ferrocenyl-chalcone unit, $H_a$ and $H_b$ resonate as two separate triplets at $\delta$ −1.77 and −0.38, respectively. These signals appear at very upfield positions due to the shielding effect of the phthalocyanine ring. With reference to the $^1$H NMR spectrum of symmetrical phthalocyanine **4.11a** (see Appendix 24) and the $^1$H−$^1$H COSY spectrum of **5.9** (see Appendix 32 for the full spectrum), the signals for $H_c$ and $H_d$ are masked by the signal of residual water in $CDCl_3$ and the multiplets at $\delta$ 3.43–3.62, respectively. The four sets of doublets in between $\delta$ 6.81 and 7.91 correspond to the aromatic ($H_f$ and $H_g$) and vinyl protons ($H_h$ and $H_i$) of the ligand. As revealed by the coupling constants ($J$), the signals resonated at $\delta$ 7.08 and 7.73 are due to the vinyl protons ($J$ = 15.2 and 15.6 Hz, respectively), whereas the signals at $\delta$ 6.81 and 7.91 correspond to the aromatic protons ($J$ = 8.8 Hz). This assignment was further supported by

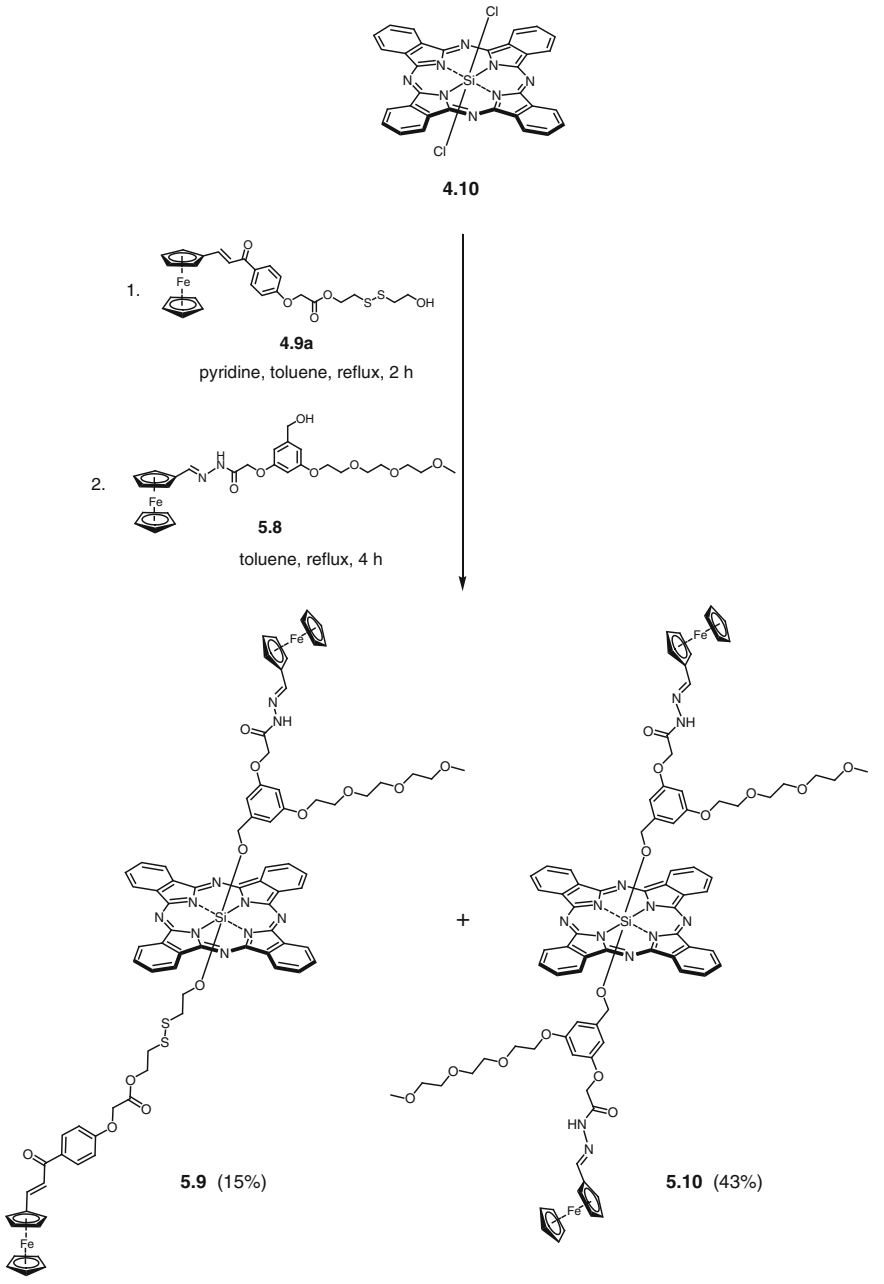


**Scheme 5.2** Synthesis of silicon(IV) phthalocyanines **5.9** and **5.10**

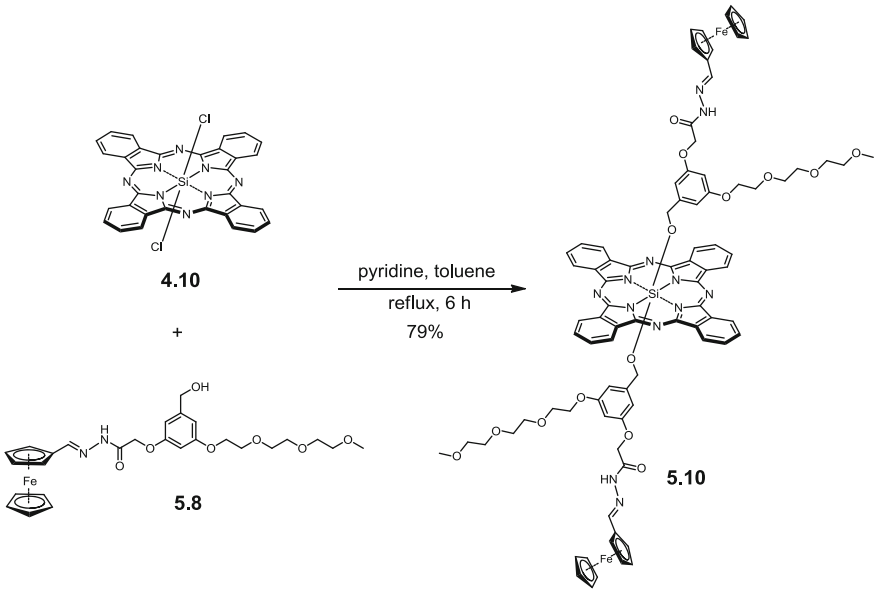


**Scheme 5.3** Synthesis of silicon(IV) phthalocyanine **5.10**

the $^1$H−$^1$H COSY spectrum in which two sets of correlated signals are observed (Fig. 5.2a). By taking reference to the $^1$H NMR spectrum of **4.11a**, the singlet (2H) at $\delta$ 4.39 can be assigned to $H_e$. Since $H_e$ does not couple with any nearby protons, it resonates as an isolated signal in the $^1$H–$^1$H COSY spectrum (Fig. 5.2b). For the ferrocenylcarbonylhydrazone unit, the signal for $H_1$ is shifted upfield as a singlet at $\delta$ −0.70 due to the phthalocyanine ring current effect. Similarly, aromatic protons $H_2$, $H_3$, and $H_4$ are also shifted upfield. The strong singlet (3H) at $\delta$ 3.36 and the multiplets at $\delta$ 3.43–3.62 (14H, of which 2H belong to $H_d$) are assigned to the methyl and methylene protons of the triethylene glycol chain, respectively. The three distinct singlets at $\delta$ 3.83, 8.00, and 8.74 can be unambiguously assigned to the methylene proton $H_5$, imine proton $H_7$, and amide proton $H_6$, respectively, with reference to the $^1$H NMR spectrum of **5.10** (see Appendix 33). As the two ferrocene units of **5.9** locate at two different electronic environments, it is expected that each of them resonates as two sets of signals with three singlets in a ratio of 2:2:5, which is typical for a monosubstituted ferrocene. The assignment is also confirmed by two sets of correlated signals as shown in the $^1$H−$^1$H COSY spectrum (Fig. 5.2b).

## *5.2.2 Electronic Absorption and Photophysical Properties*

Figure 5.3 shows the electronic absorption spectra of phthalocyanines **5.9** and **5.10** in DMF. These spectra are typical for non-aggregated phthalocyanines with a B-band at 354 nm, an intense and sharp Q-band at 677–678 nm, together with two

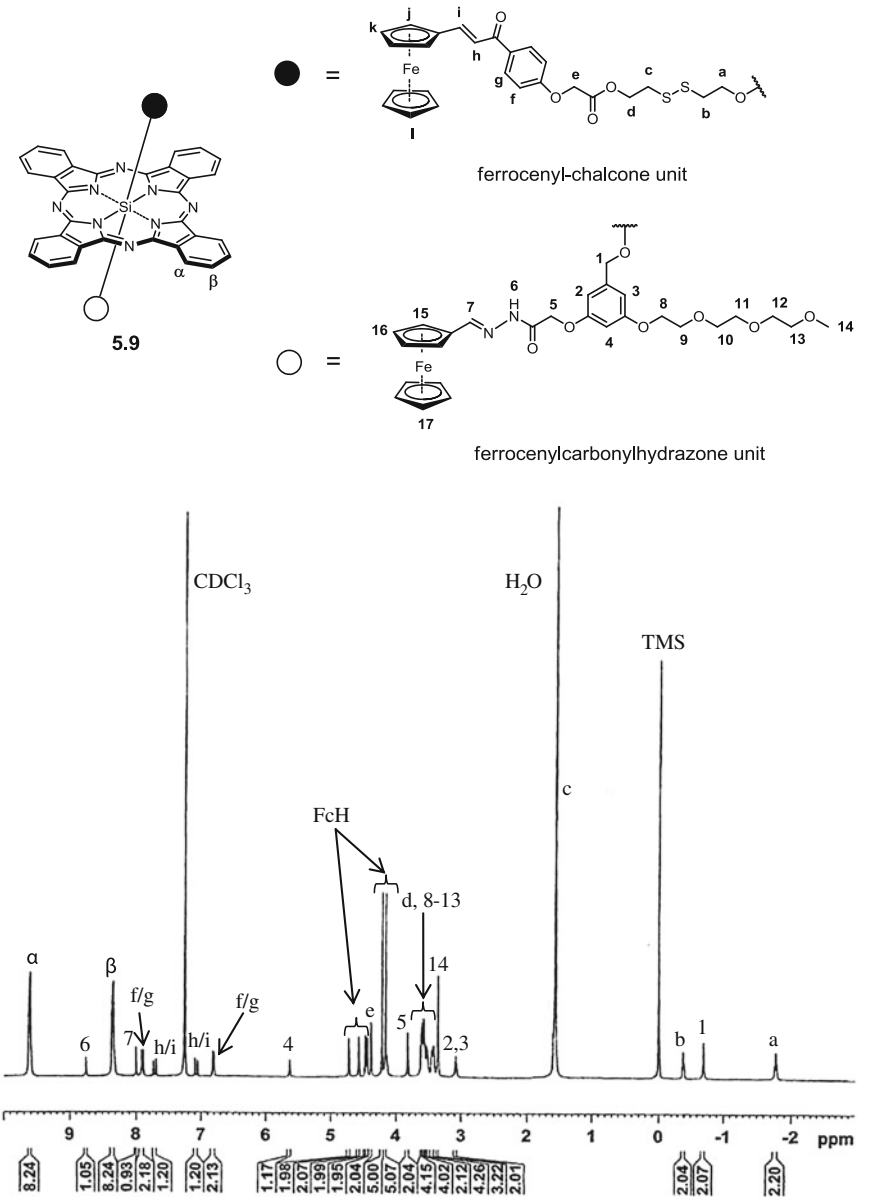


**Fig. 5.1** $^{1}$H NMR spectrum of **5.9** in $CDCl_3$

vibronic bands at 608–611 and 646–647 nm (Table 5.1). For the unsymmetrical phthalocyanine **5.9**, two additional bands at 330 and 496 nm, probably due to the absorption of the $\pi$-conjugated ferrocenyl-chalcone system, were also recorded. In fact, a similar phenomenon has been observed for phthalocyanines **4.11a** and **4.11b**

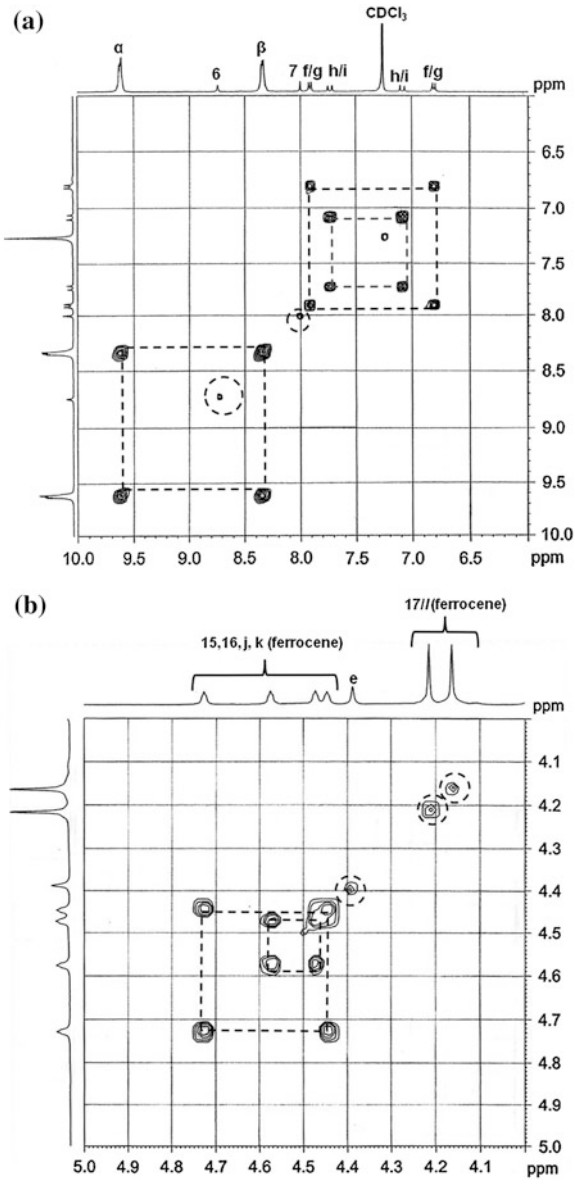


**Fig. 5.2** $^{1}H-^{1}H$ COSY spectrum of **5.9** in $CDCl_3$. (*Dotted squares* and *circles* denote correlated and isolated signals, respectively.)

as described in Chap. 4. Upon excitation at 610 nm, these phthalocyanines showed a fluorescence emission at 687–688 nm. Due to the quenching effect of the singlet excited state of the phthalocyanines by the ferrocenyl moieties, they displayed relatively low fluorescence quantum yields ($\Phi_F = 0.03$-$0.05$) relative to unsubstituted zinc(II) phthalocyanine (ZnPc) in DMF ($\Phi_F = 0.28$) (Table 5.1) [23]. These values are comparable to the values for **4.11a** and **4.11b** (see Table 4.1).

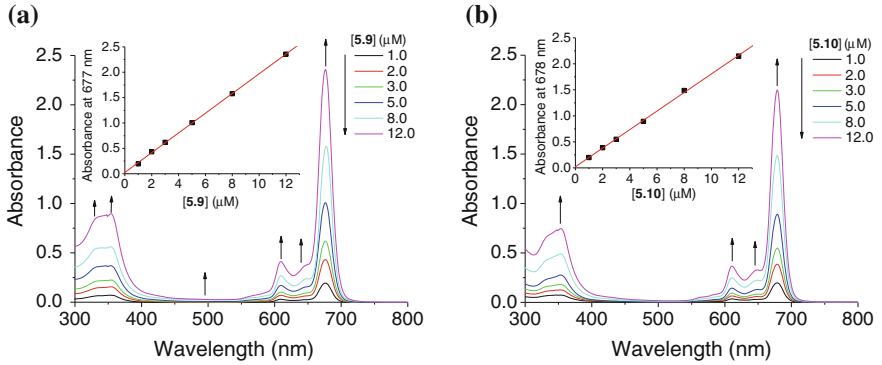


**Fig. 5.3** Electronic absorption spectra of (**a**) **5.9** and (**b**) **5.10** in different concentrations in DMF. The inset plots the Q-band absorbance versus the concentration of the phthalocyanine, and the line represents the best-fitted straight line

To evaluate the photosensitizing efficiency of phthalocyanines **5.9** and **5.10**, their singlet oxygen quantum yields ($\Phi_\Delta$) were determined by a steady-state method with 1,3-diphenylisobenzofuran (DPBF) as the scavenger in DMF. The changes in concentration of the quencher were monitored spectroscopically at 411 nm with time (Fig. 5.4), from which the values of $\Phi_\Delta$ could be determined by the method described previously [18]. Both phthalocyanines could generate singlet oxygen ($\Phi_\Delta = 0.07-0.10$), but the efficiency was much lower than that of ZnPc ($\Phi_\Delta = 0.56$) (Table 5.1) [18]. The relatively low singlet oxygen quantum yields of **5.9** and **5.10** may also be attributed to the quenching effect by the ferrocenyl moieties, which disfavor intersystem crossing and eventually the formation of singlet oxygen. A similar phenomenon has also been observed for **4.11a** and **4.11b** as described in Chap. 4.

In order to gain a better understanding on the aggregation behavior of the phthalocyanines in the biological environment, their electronic absorption and fluorescence spectra were also recorded in the Roswell Park Memorial Institute (RPMI) 1640 culture medium with 0.5 % Cremophor EL. As shown in Fig. 5.5a, both phthalocyanines display a sharp and intense Q-band, indicating that they are essentially non-aggregated in the culture medium. Their corresponding fluorescence spectra in the same condition are shown in Fig. 5.5b. To demonstrate the quenching effect exerted by the ferrocenyl moieties, the spectra of **4.11a** and **4.12** are also included for comparison. Among these four compounds, **4.12** shows the greatest fluorescence intensity since the two ferrocenyl moieties are absent in this compound. As expected, the three ferrocenyl phthalocyanines **4.11a**, **5.9**, and **5.10** show very weak fluorescence intensity due to the quenching effect, particularly for **5.10**, which has the shortest separation between two the quencher and the phthalocyanine ring.

**Table 5.1** Electronic absorption and photophysical data for **5.9** and **5.10** in DMF

| Compound | $\lambda_{max}$ (nm) (log $\varepsilon$) | $\lambda_{em}$(nm)[a] | $\Phi^{b}_{F}$ | $\Phi^{c}_{\Delta}$ |
|---|---|---|---|---|
| **5.9** | 330 (4.84), 354 (4.86), 496 (3.47), 608 (4.53), 646 (4.49), 677 (5.29) | 687 | 0.05 | 0.10 |
| **5.10** | 354 (4.79), 611 (4.48), 647 (4.43), 678 (5.25) | 688 | 0.03 | 0.07 |

[a] Excited at 610 nm. [b] Using ZnPc in DMF as the reference ($\Phi_F = 0.28$). [c] Using ZnPc as the reference ($\Phi_\Delta = 0.56$ in DMF)

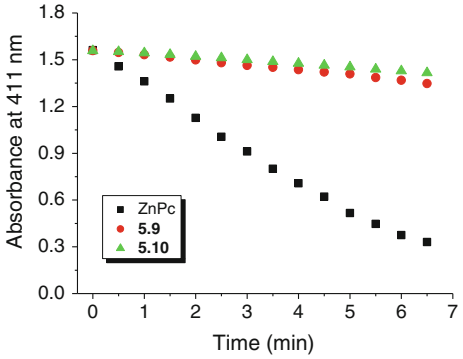


**Fig. 5.4** Comparison of the rates of decay of DPBF (initial concentration = 70 μM) sensitized by **5.9**, **5.10**, and **ZnPc** (all at 3 μM) in DMF as shown by the decrease in the absorbance at 411 nm

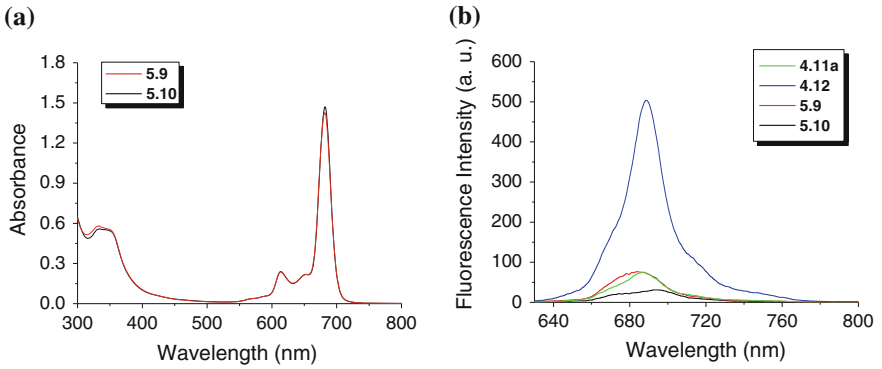


**Fig. 5.5** (**a**) Electronic absorption spectra of **5.9** and **5.10** in the RPMI culture medium with 0.5 % Cremophor EL (both at 8 μM). The fluorescence spectra ($\lambda_{ex} = 610$ nm) of **4.11a**, **4.12**, **5.9**, and **5.10** under the same conditions are shown in (**b**)

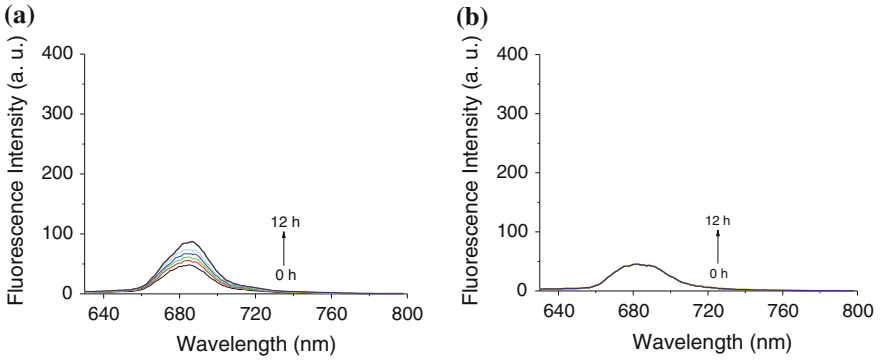


**Fig. 5.6** Changes in fluorescence spectra ($\lambda_{ex} = 610$ nm) of (**a**) **5.9** and (**b**) **5.10** (both at 4 μM) in the presence of 10 mM DTT in PBS with 0.5 % Cremophor EL with time

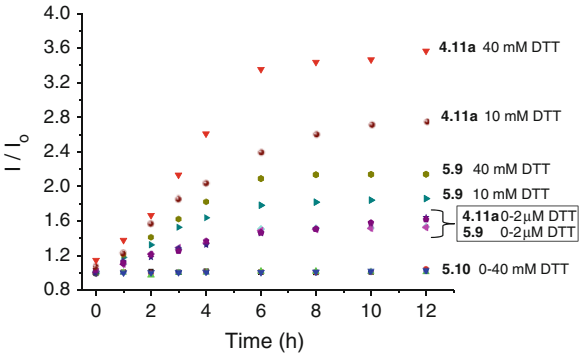


**Fig. 5.7** Changes in fluorescence intensities of **4.11a**, **5.9**, and **5.10** (all at 4 μM) toward different concentrations of DTT in PBS with 0.5 % Cremophor with time

## *5.2.3 pH- and Redox-Responsive Properties*

To investigate the pH- and redox-responsive properties of these phthalocyanines, their fluorescence response toward different concentrations of dithiothreitol (DTT), and different pH in phosphate buffered saline (PBS) was first studied. For comparison, the response of the redox-sensitive phthalocyanine **4.11a** and the non-cleavable control **4.11b** is also included.

### 5.2.3.1 Fluorescence Response to DTT

The redox-responsive properties of **4.11a**, **5.9**, and **5.10** were evaluated by monitoring their changes in fluorescence intensity with different DTT concentrations against time. In Chap. 4, we have reported the time-dependent changes in fluorescence spectra of **4.11a** and **4.11b** at different concentrations of DTT in PBS (Fig. 4.4). In the present investigation, we have also performed a similar study to

examine the effect of DTT on the fluorescence intensities of **5.9** and **5.10.** Figure 5.6 shows the time-dependent changes in fluorescence intensities of **5.9** and **5.10** in PBS with 10 mM DTT for exemplification. Figure 5.7 summarizes the time-dependent changes in fluorescence intensities of all the phthalocyanines upon exposure to different concentrations of DTT in PBS. It can be seen that phthalocyanine **4.11a** shows the greatest enhancement in fluorescence intensity in the presence of 10 or 40 mM DTT as a result of the disulfide bond cleavage. As expected, compound **5.10** shows negligible changes in fluorescence intensity as the acid-labile hydrazone linkers are not responsive to a reducing stimulus. For the unsymmetrical phthalocyanine **5.9**, it shows moderate fluorescence enhancement in the presence of 10 or 40 mM DTT. The moderate increase in fluorescence intensity is attributed to the cleavage of the disulfide bond, thus releasing one ferrocenyl moiety. Since the singlet excited state is still partially quenched by the ferrocenylcarbonylhydrazone moiety, the fluorescence intensity enhancement was not as significant as **4.11a** under the same experimental condition. Upon addition of 2 μM DTT, which mimics the extracellular environment, the fluorescence intensities of both **4.11a** and **5.9** only increase slightly.

In order to examine the aggregation behavior of these phthalocyanines during the kinetic study, their respective Q-band was monitored over 12 h. As shown in Fig. 5.8, the Q-bands remained relatively sharp and intense, suggesting that the phthalocyanine fragment formed after cleavage of the disulfide bond of **5.9** and compound **5.10** are essentially non-aggregated throughout the study.

#### 5.2.3.2 Fluorescence Response to pH

The effect of pH on the fluorescence emission of **4.11a**, **5.9**, and **5.10** was also examined. Figure 5.9 shows the time-dependent changes in fluorescence spectra of **5.10** in PBS at pH 4.5, 6.0, and 7.4, which were used to mimic the tumor lysosomal compartment, tumor interstitial environment, and extracellular environment of normal tissues, respectively. It can be seen that the fluorescence increases to a greater extent at lower pH. Figure 5.10 summarizes the corresponding time-dependent changes in fluorescence intensities of **4.11a**, **5.9**, and **5.10** in PBS at the above pH values. For compound **5.10**, there are no significant changes in the fluorescence intensity over 12 h at pH 7.4, while its fluorescence intensity increases significantly at pH 4.5 and 6.0. The enhancement of fluorescence intensities at pH 4.5 and 6.0 is attributed to the hydrolytic cleavage of the hydrazone bond, thus releasing the ferrocenyl moieties and inhibiting the quenching effect. The fluorescence intensity of **5.10** increases by about 6-fold when the pH decreases from 7.4 to 4.5. For the unsymmetrical phthalocyanine **5.9**, it shows moderate increase in fluorescence intensity at pH 4.5 and 6.0 due to the release of only one ferrocenyl moiety. As the singlet excited state of the phthalocyanine is still partially quenched by the remaining ferrocenyl-chalcone moiety after cleavage of the hydrazone bond, the fluorescence intensity enhancement is not as drastic as **5.10** under the same experimental condition. For compound **4.11a**,

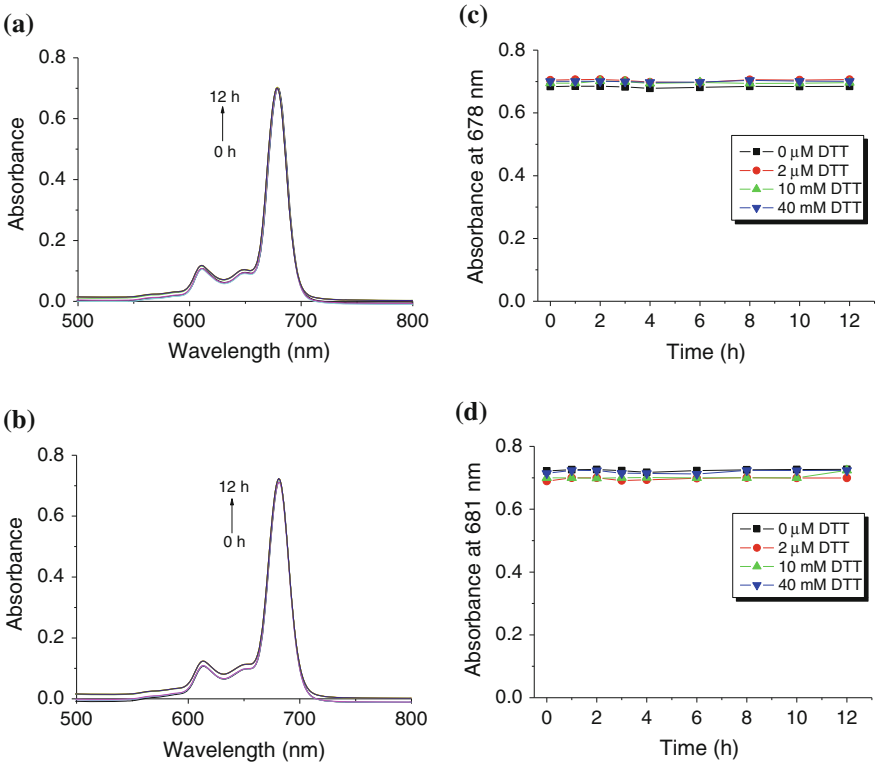


**Fig. 5.8** Changes in absorption spectra of (**a**) **5.9** and (**b**) **5.10** (both at 4 μM) upon exposure to 40 mM DTT in PBS with 0.5 % Cremophor EL with time. The changes in Q-band absorbance upon exposure to 0-40 mM DTT with time are shown in (**c**) and (**d**) for **5.9** and **5.10**, respectively

which does not possess any pH-responsive linkages, no significant fluorescence enhancement was observed at pH 4.5 to 7.4. Similarly, the Q-band of these compounds remained sharp and intense during the 12-hour kinetic study (data not shown). The results suggest that these compounds or their phthalocyanine fragments are essentially non-aggregated throughout the study.

### 5.2.3.3 Fluorescence Response to DTT and pH

We proceeded to examine the time-dependent changes of fluorescence intensities of **4.11a**, **4.11b**, **5.9**, and **5.10** in PBS at pH 6.0 or 7.4 in the presence of 2 μM or 10 mM DTT (Fig. 5.11). For the redox-responsive phthalocyanine **4.11a**, enhancement in fluorescence intensity was observed in a higher DTT concentration (10 mM) and was independent of the change in pH (Fig. 5.11a). By contrast, the fluorescence enhancement of the pH-responsive analogue **5.10** was observed when the pH was changed from 7.4 to 6.0 regardless the concentration of DTT

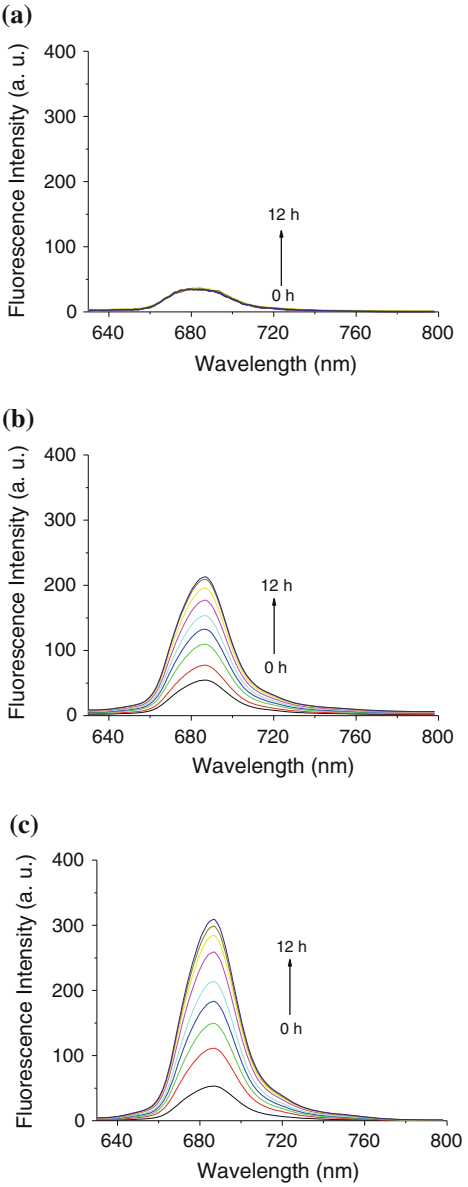


**Fig. 5.9** Changes in fluorescence spectra ($\lambda_{ex} = 610$ nm) of **5.10** (4 μM) in PBS (with 0.5 % Cremophor) at different pH (4.5, 6.0, and 7.4) with time

(Fig. 5.11d). For the unsymmetrical phthalocyanine **5.9**, the fluorescence enhancement was most significant when it was exposed to pH 6.0 and 10 mM DTT, while the response was comparatively less significant at either low pH or high DTT concentration. The fluorescence increase was minimal at pH 7.4 and 2 μM DTT (Fig. 5.11c). These observations suggest that both the disulfide and hydrazone linkages of **5.9** are cleaved in the presence of 10 mM DTT at pH 6.0,

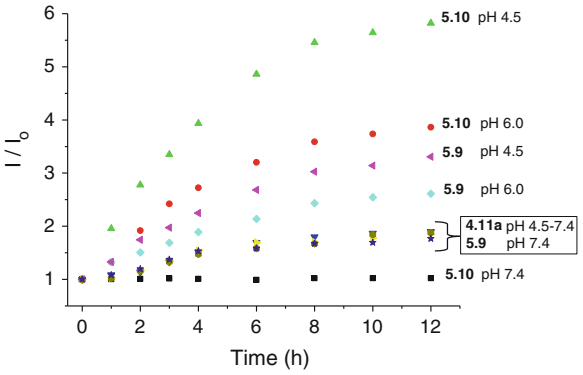


**Fig. 5.10** Changes in fluorescence intensities of **4.11a**, **5.9**, and **5.10** (all at 4 μM) in PBS (with 0.5 % Cremophor) at different pH (4.5, 6.0, and 7.4) with time

releasing the two ferrocenyl moieties, thereby minimizing the quenching effect and restoring the fluorescence intensity. As expected, for the non-cleavable control **4.11b**, there were negligible changes in fluorescence intensities at all these conditions (Fig. 5.11b). As revealed by the sharp and intense Q-band of these phthalocyanines (data not shown), these compounds and their fragments remained essentially non-aggregated throughout the kinetic study.

#### 5.2.3.4 Effect of DTT on Singlet Oxygen Production

Apart from fluorescence response, the effects of DTT and pH on the efficiency of singlet oxygen generation of **5.9** and **5.10** in PBS were also studied. For comparison, the response of **4.11a** was also included. Figure 5.12 compares the rates of decay of DPBF sensitized by **4.11a**, **5.9**, and **5.10** upon exposure to different concentrations of DTT for 8 h in PBS. All these phthalocyanines could not induce singlet oxygen generation in the dark even in the presence of 10 mM DTT (data not shown). Upon illumination and at 2 μM DTT, which was used to mimic the extracellular reducing environment, all these phthalocyanines could produce a small amount of singlet oxygen. In the presence of 10 mM DTT, which mimics the intracellular reducing environment, the singlet oxygen production efficiency of **4.11a** and **5.9** increased remarkably. The enhancement in singlet oxygen generation could be ascribed to the reductive cleavage of the disulfide bonds, resulting in restoration of the photosensitizing property. Since **5.9** still contains the ferrocenylcarbonylhydrazone moiety after cleavage of the disulfide bond, the singlet oxygen generation efficiency of **5.9** is lower than that of **4.11a**. For **5.10**, which does not contain disulfide linkages, the singlet oxygen production was minimal even in the presence of 10 mM DTT.

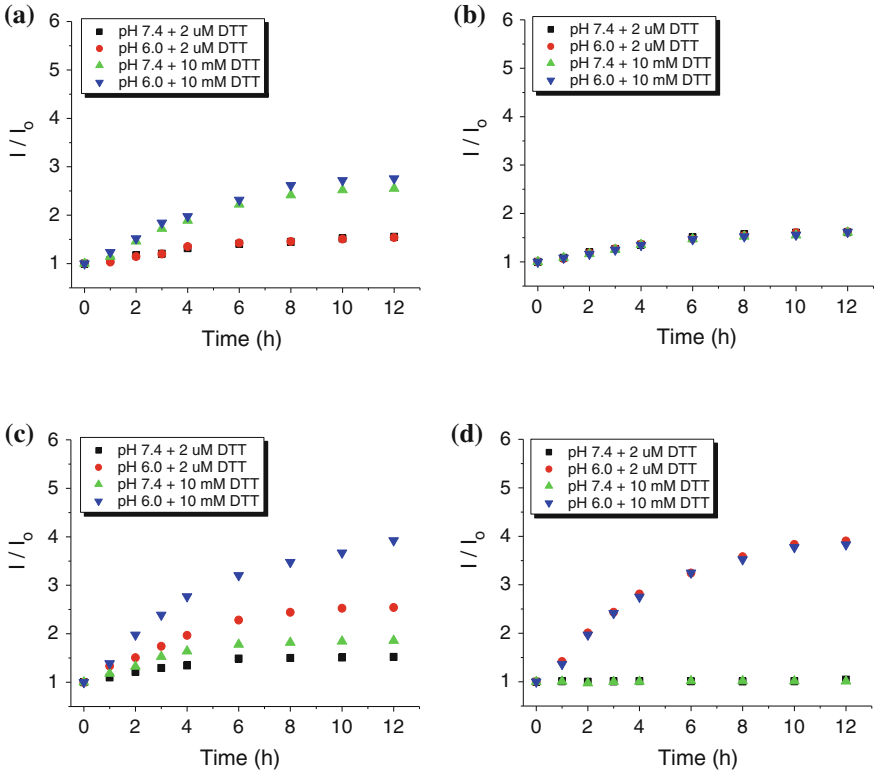


**Fig. 5.11** Time-dependent changes in fluorescence intensities of (**a**) **4.11a**, (**b**) **4.11b**, (**c**) **5.9**, and (**d**) **5.10** (all at 4 μM) in PBS (with 0.5 % Cremophor) at pH 6.0 or 7.4 and in the presence of 2 μM or 10 mM DTT

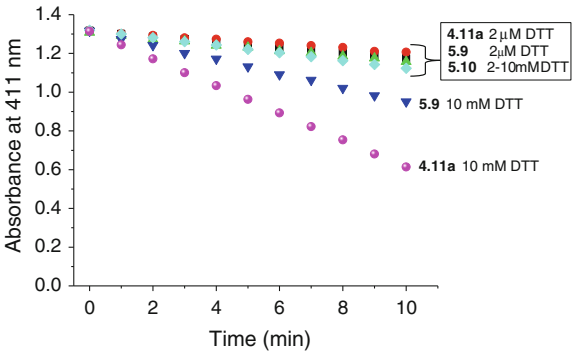


**Fig. 5.12** Comparison of the rates of decay of DPBF (initial concentration = 70 μM) sensitized by **4.11a**, **5.9**, and **5.10** (all at 4 μM) upon exposure to different concentrations of DTT for 8 h in PBS with 0.5 % Cremophor EL

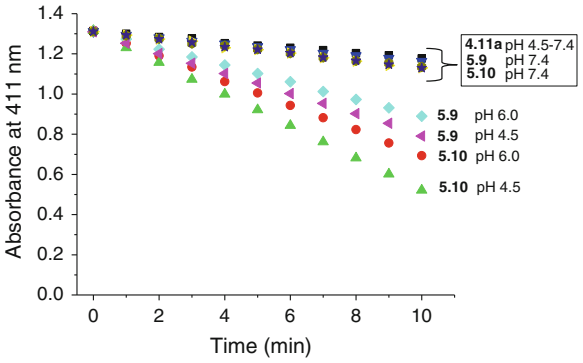


**Fig. 5.13** Comparison of the rates of decay of DPBF (initial concentration = 70 μM) sensitized by **4.11a**, **5.9**, and **5.10** (all at 4 μM) in PBS with 0.5 % Cremophor EL at different pH (4.5, 6.0, and 7.4) for 8 h in the presence of light ($\lambda > 610$ nm)

### 5.2.3.5 Effect of pH on Singlet Oxygen Production

The effects of pH on the production of singlet oxygen of these phthalocyanines were also examined. Figure 5.13 compares the rates of decay of DPBF induced by these phthalocyanines in PBS at different pH (4.5, 6.0, and 7.4) for 8 h. In the absence of light, all these phthalocyanines could not sensitize the production of singlet oxygen (data not shown). At pH 7.4, they could slightly produce singlet oxygen upon illumination. Under a mildly acidic condition (pH 6.0), both **5.9** and **5.10** showed an increase in the production of singlet oxygen. The singlet oxygen generation efficiency was further enhanced when the pH was decreased to 4.5. Such an increase in singlet oxygen generation could be attributed to the hydrolysis of the hydrazone linkers under acidic conditions, thus releasing the ferrocenyl moieties and reducing the quenching effect. Since **5.9** still contains a ferrocenyl-chalcone moiety after cleavage of the hydrazone bond, its singlet oxygen generation efficiency is lower than that of **5.10** at the same pH. As expected, the control **4.11a** is not responsive to pH due to the absence of acid-labile linkages. These results demonstrate that compound **5.10** is also a promising tumor-selective photosensitizer as it exhibits remarkably different fluorescence emission and singlet oxygen generation properties at pH 4.5, 6.0, and 7.4, which are the general pH environments for tumor lysosomal compartments, tumor interstitium, and normal tissues, respectively [11, 12, 27].

### 5.2.3.6 Effect of DTT and pH on Singlet Oxygen Production

To show the effects of pH and DTT on the singlet oxygen generation efficiency of these compounds, we also compared the rates of decay of DPBF induced by these phthalocyanine in PBS at pH 6.0 or 7.4 and in the presence of 2 μM or 10 mM DTT for 8 h (Fig. 5.14). In the absence of light, these phthalocyanines could not produce singlet oxygen (data not shown). Upon illumination, these phthalocyanines exhibited different extent of singlet oxygen generation efficiency. For the redox-responsive phthalocyanine **4.11a**, the singlet oxygen generation efficiency was increased only

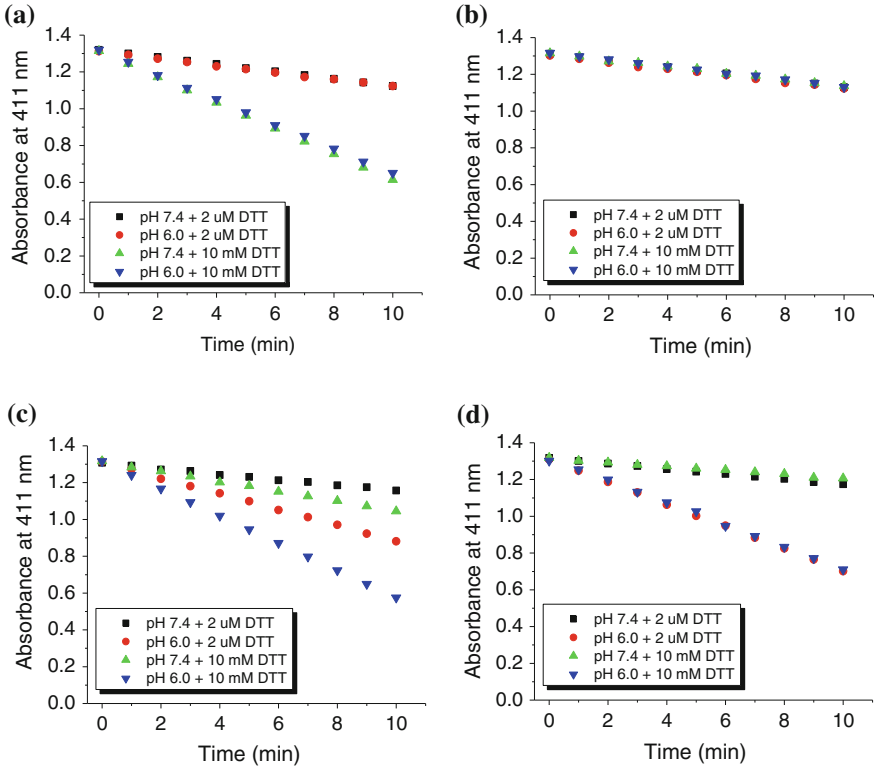


**Fig. 5.14** Comparison of the rates of decay of DPBF (initial concentration = 70 μM) sensitized by (**a**) **4.11a**, (**b**) **4.11b**, (**c**) **5.9**, and (**d**) **5.10** (all at 4 μM) in PBS with 0.5 % Cremophor EL at different pH (6.0 and 7.4) for 8 h in the presence of light ($\lambda > 610$ nm)

when the DTT concentration was increased from 2 μM to 10 mM (Fig. 5.14a). On the other hand, the singlet oxygen generation efficiency of the pH-responsive derivative **5.10** increased only when the pH decreased from 7.4 to 6.0 (Fig. 5.14d). For the unsymmetrical phthalocyanine **5.9**, the production of singlet oxygen was the greatest at pH 6.0 and in the presence of 10 mM DTT, while the efficiency was comparatively lower at either low pH or high DTT concentration (Fig. 5.14c). As expected, the non-cleavable control **4.11b** could not cause any singlet oxygen generation enhancement under all these conditions (Fig. 5.14b).

### *5.2.4 In Vitro Photodynamic Activities*

The pH- and redox-dependent fluorescence emission of unsymmetrical phthalocyanine **5.9** at the cellular level was also examined. In this study, MCF-7 human breast cancer cells were first pretreated with different concentrations of DTT

(0–4 mM) for 1 h, followed by incubation with the ionophore nigericin at two different pH (5.0 or 7.4) for 30 min. Nigericin is an $H^+/K^+$ antiporter, which enables the electroneutral transport of extracellular $H^+$ ions in exchange for intracellular $K^+$ ions, and can equilibrate the intracellular and extracellular pH [13, 28]. After the cells were treated with **5.9** (1 μM) for a further 1 h, the corresponding fluorescence images of the cells were captured with a confocal microscope (Fig. 5.15a), and the intracellular fluorescence intensities were determined (Fig. 5.15b). As shown in Fig. 5.15, very weak fluorescence was observed when the cells were exposed to 0–2 μM DTT at pH 7.4. However, the fluorescence intensity increased by about 3-fold when the DTT concentration was increased to 4 mM. This can be attributed to the cleavage of the disulfide bond and the separation of the ferrocenyl-chalcone moiety from the phthalocyanine partially relieved the quenching effect, leading to an enhancement in intracellular fluorescence intensity. At pH 5.0, the cells showed moderate intracellular fluorescence in the presence of 0–2 μM DTT due to the cleavage of the acid-labile linker and the release of ferrocenyl moiety. The intracellular fluorescence under this condition was stronger when compared with that exposed to 4 mM DTT at pH 7.4. It is likely that after the cleavage of the acid-labile hydrazone linker, the quenching effect induced by the remaining disulfide-linked ferrocene is not as efficient as the hydrazone-linked ferrocene due to the longer distance between the phthalocyanine ring and the ferrocenyl moiety, and hence relatively higher fluorescence intensity was observed. The fluorescence intensity was particularly strong when the cells were exposed to 4 mM DTT at pH 5.0, under which both disulfide and hydrazone linkages are cleaved, rendering the compound to be fully "turned on". Considering the fact that these conditions are analogous to the reducing and low pH environment as in the tumor, the results suggest that **5.9** is a potential dual pH- and redox-responsive photosensitizer for targeted PDT.

The pH-dependent fluorescence emission of **5.10** was also investigated. The MCF-7 cells were first incubated with nigericin at three different pH environments (5.0, 6.0, or 7.4) for 30 min, followed by incubation with **5.10** for 1 h. As shown in Fig. 5.16, the intracellular fluorescence intensities are much stronger at pH 5.0 and 6.0 than that at pH 7.4 (by about 9- to 10-fold). On the basis that the general pH environments for tumors and normal tissues fall in this region (from 6.0 to 7.4) [11, 27], the results suggest that compound **5.10** is also a promising pH-controlled photosensitizer for targeted PDT.

The photodynamic activities of phthalocyanines **5.9** and **5.10** were also evaluated against MCF-7 cells. To demonstrate the effect of reducing stimulus on the cytotoxicity, the cells were pretreated with DTT (2 μM or 4 mM) for 1 h, prior to incubation with the phthalocyanine solutions for 6 h. Figure 5.17 shows the dose-dependent survival curves for these two compounds with different concentrations of DTT in the absence and presence of light. Both compounds are essentially non-cytotoxic in the absence of light regardless of the concentration of DTT, but exhibit high photocytotoxicity. The $IC_{50}$ values are summarized in Table 5.2. In the presence of light, the photocytotoxicity of **5.9** remains nearly unchanged in the absence and presence of 2 μM DTT. However, the antiproliferative effect is

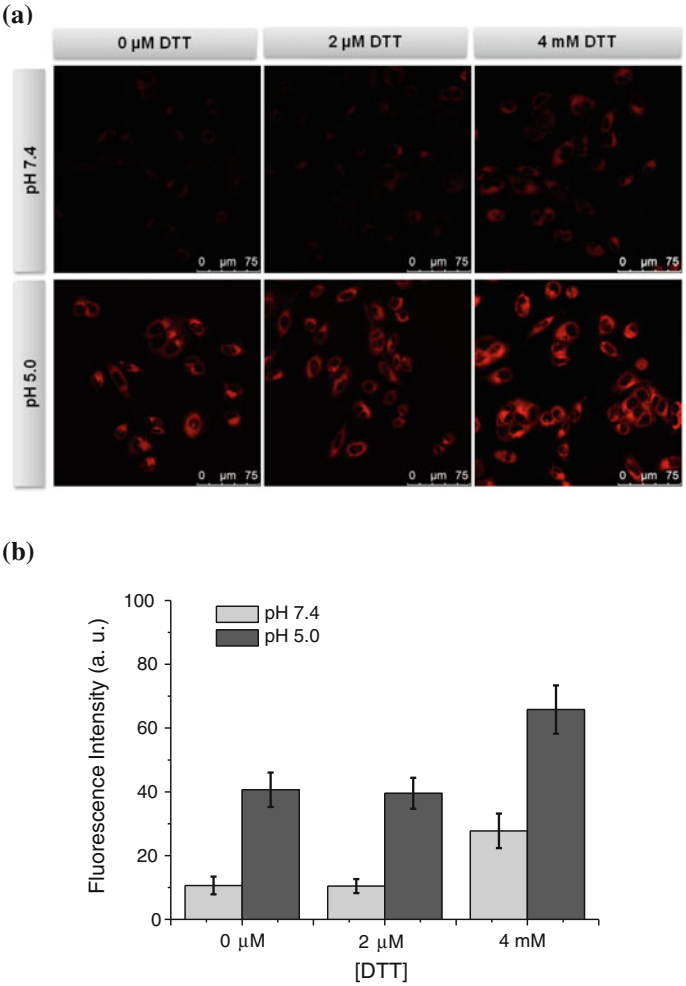


**Fig. 5.15** (**a**) Fluorescence images of MCF-7 cells after incubation with 0–4 mM DTT for 1 h and then with nigericin (at pH 5.0 or 7.4) for 30 min, followed by incubation with **5.9** (1 μM) for 1 h. (**b**) Comparison of the relative intracellular fluorescence intensity of **5.9** at different DTT concentrations and pH values. Data are expressed as mean value ± standard deviation (S.D.) (number of cells = 30)

greatly enhanced when the DTT concentration is increased to 4 mM with $IC_{50}$ value as low as 64 nm. The enhancement in photocytotoxicity can be attributed to the cleavage of the disulfide bond, thus releasing one ferrocenyl moiety and partially relieving the quenching effect. Compound **5.10** is highly potent with $IC_{50}$ values in the range of 73–75 nM. It can be seen that its photocytotoxicity is independent of the concentrations of DTT.

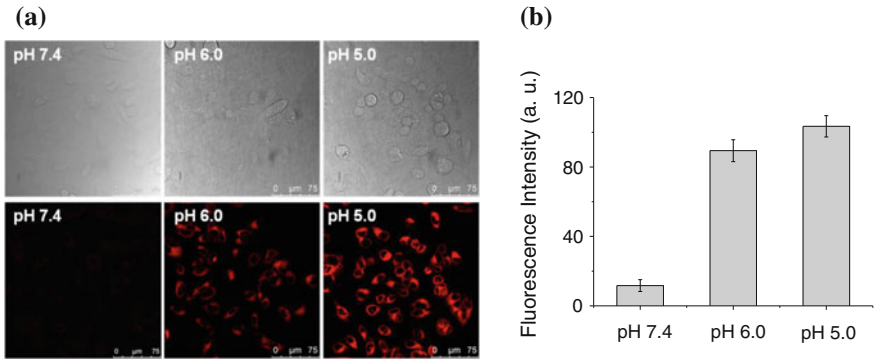


**Fig. 5.16** (**a**) Fluorescence images of MCF-7 cells after incubation with a nigericin solution (25 μM) at pH 5.0, 6.0, or 7.4 for 30 min, followed by incubation with **5.10** (1 μM) for 1 h. The corresponding bright field images are shown in the upper row. (**b**) Comparison of the relative intracellular fluorescence intensity of **5.10** in the presence of nigericin at different pH values. Data are expressed as mean value ± S.D. (number of cells = 30)

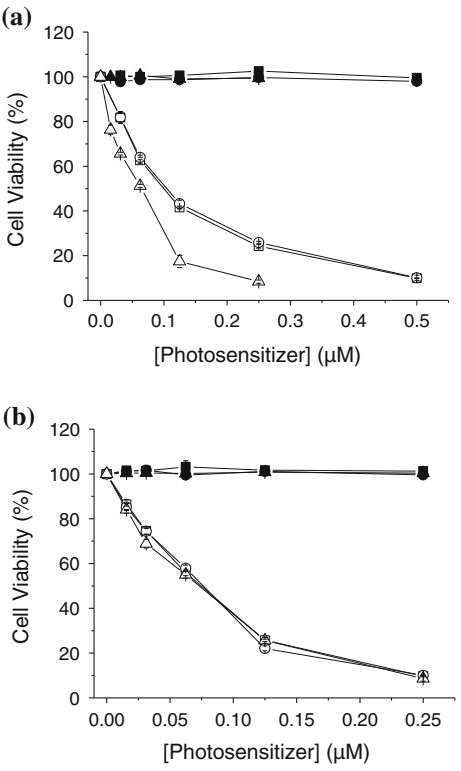


**Fig. 5.17** Cytotoxic effects of (**a**) **5.9** and (**b**) **5.10** on MCF-7 cells pretreated with 0 μM (*squares*), 2 μM (*circles*), and 4 mM (*triangles*) DTT, prior to drug incubation for 6 h in the absence (*closed symbols*) and presence (*open symbols*) of light ($\lambda > 610$ nm, 40 mW $cm^{-2}$, 48 J $cm^{-2}$). Data are expressed as mean value ± standard error of the mean (S.E.M.) of three independent experiments, each performed in quadruplicate

**Table 5.2** $IC_{50}$ values for phthalocyanines **5.9** and **5.10** on MCF-7 cells

| Compound | $IC_{50}$ (nM) | | |
|---|---|---|---|
| | 0 μM DTT | 2 μM DTT | 4 mM DTT |
| **5.9** | 100 | 105 | 64 |
| **5.10** | 75 | 76 | 73 |

The pH-dependent photocytotoxicity study of **5.9** and **5.10** against MCF-7 cells was not performed. Based on our previous results, most of the cells were killed when they were maintained in an acidic medium (e.g. pH = 6.5) for 2–3 h even in the absence of the phthalocyanines. Therefore, the study could not give any meaningful and conclusive results.

## 5.3 Summary

In summary, we have prepared and characterized a dual pH- and redox-responsive silicon(IV) phthalocyanine **5.9.** The fluorescence intensity and singlet oxygen generation efficiency of this compound are enhanced in a slightly acidic condition or in the presence of DTT (4 mM). The enhancement is particularly significant when the compound is exposed to an environment at low pH value and with a high level of DTT, which is analogous to the acidic and reducing environment found in tumor tissues. In addition, we have also described a pH-responsive silicon(IV) phthalocyanine **5.10**, which also shows pH-dependent properties in fluorescence emission and singlet oxygen generation. In the pH range of ca. 5–7, which can differentiate the environments for tumors and normal tissues, it shows stronger fluorescence emission and behaves as a more efficient singlet oxygen generator at lower pH. These pH- and/or redox-responsive properties render compounds **5.9** and **5.10** highly promising tumor-selective photosensitizers for targeted PDT.

## References

1. Arnbjerg, J., Johnsen, M., Nielsen, C.B., Jørgensen, M., Ogilby, P.R.J.: Phys. Chem. A **111**, 4573 (2007)
2. Bae, Y., Fukushima, S., Harada, A., Kataoka, K.: Angew. Chem. Int. Ed. **42**, 4640 (2003)
3. Bellnier, D.A., Young, D.N., Detty, M.R., Camacho, S.H., Oseroff, A.R.: Photochem. Photobiol. **70**, 630 (1999)
4. Blair, S.L., Heerdt, P., Sacher, S., Abolhoda, A., Hochwald, S., Cheng, H., Burt, M.: Cancer Res. **57**, 152 (1997)
5. Chen, J., Qiu, X., Ouyang, J., Kong, J., Zhong, W., Xing, M.M.Q.: Biomacromolecules **12**, 3601 (2011)
6. Cook, J.A., Pass, H.I., Iype, S.N., Friedman, N., Degraff, W., Russo, A., Mitchell, J.B.: Cancer Res. **51**, 4287 (1991)

7. Cunderliková, B., Bjørklund, E.G., Pettersen, E.O., Moan, J.: Photochem. Photobiol. **74**, 246 (2001)
8. Cunderliková, B., Moan, J., Sjaastad, I.: Cancer Lett. **222**, 39 (2005)
9. Friberg, E.G., Cunderliková, B., Pettersen, E.O., Moan, J.: Cancer Lett. **195**, 73 (2003)
10. Gao, L., Fei, J., Zhao, J., Cui, W., Cui, Y., Li, J.: Chem. Eur. J. **18**, 3185 (2012)
11. Gerweck, L.E.: Drug Resist. Updates **3**, 49 (2000)
12. Gerweck, L.E., Seetharaman, K.: Cancer Res. **56**, 1194 (1996)
13. Jähde, E., Glüsenkamp, K.-H., Rajewsky, M.F.: Cancer Chemother. Pharmacol. **27**, 440 (1991)
14. Jiang, X.-J., Lo, P.-C., Yeung, S.-L., Fong, W.-P., Ng, D.K.P.: Chem. Commun. **46**, 3188 (2010)
15. Kosower, N.S., Kosower, E.M.: Int. Rev. Cytol. **54**, 109 (1978)
16. Lo, P.-C., Huang, J.-D., Cheng, D.Y.Y., Chan, E.Y.M., Fong, W.-P., Ko, W.-H., Ng, D.K.P.: Chem. Eur. J. **10**, 4831 (2004)
17. Loim, N.M., Kelbyscheva, E.S.: Russ. Chem. Bull. **53**, 2080 (2004)
18. Maree, M.D.; Kuznetsova, N.; Nyokong, T. J. Photochem. Photobiol., A **2001**, *140*, 117
19. Moan, J., Smedshammer, L., Christensen, T.: Cancer Lett. **9**, 327 (1980)
20. Mojzisova, H., Bonneau, S., Vever-Bizet, C., Brault, D.: Biochim. Biophys. Acta **1768**, 2748 (2007)
21. Ozlem, S., Akkaya, E.U.J.: Am. Chem. Soc. **131**, 48 (2009)
22. Pawar, G.M., Bantu, B., Weckesse, J., Blechert, S., Wurst, K., Buchmeiser, M.R.: Dalton Trans. **41**, 9043 (2009)
23. Scalise, I., Durantini, E.N.: Bioorg. Med. Chem. **13**, 3037 (2005)
24. Sharma, M., Dube, A., Bansal, H., Gupta, P.K.: Photochem. Photobiol. Sci. **3**, 231 (2004)
25. Sharma, M.; Sahu, K.; Dube, A.; Gupta, P.K. J. Photochem. Photobiol., B **2005**, *81*, 107
26. Sivakumar, S., Reddy, M.L.P., Cowley, A.H., Butorac, R.R.: Inorg. Chem. **50**, 4882 (2011)
27. Stubbs, M.; McSheehy, P.M.J.; Griffiths, J.R.; Bashford, C.L. Mol. Med. Today **2000**, 6
28. Varnes, M.E.; Bayne, M.T.; Bright, G.R. Photochem. Photobiol.**1996**, *64*, 853